

# Non-Coherent Energy Collection Approach for TOA Estimation in UWB Systems

Alberto Rabbachin, Jean-Philippe Montillet, Paul Cheong, Giuseppe T. F. de Abreu and Ian Oppermann  
Centre for Wireless Communications  
University of Oulu  
P.O.Box 4500, 90014-Oulu, Finland.  
E-mail contact: alberto.rabbachin@ee.oulu.fi

**Abstract**— This paper examines the performance of time of arrival (TOA) estimation techniques for an UWB system employing a non-coherent energy collection receiver. The performance of two different algorithms, namely, the *threshold-crossing* (TC) and the *maximum selection* (MAX) algorithms, are compared in terms of TOA estimation error. The effect of the TOA estimation error on position calculation is evaluated for the iterative Davidon-Fletcher-Powell (DFP) quasi-Newton algorithm. It is found that the TOA estimation algorithms examined lead to similar results when applied to positioning.

## I. INTRODUCTION

One of the most attracting characteristics of ultra-wideband impulse radio (UWB-IR) is the fine time resolution proportioned by its impulsive signals, which makes impulse-based UWB a prominent candidate technology for indoor positioning systems. In general, positioning techniques exploit one or more characteristics of the radio signals to estimate the position of their sources. Some of the parameters that have been traditionally used for positioning are the received signal strength intensity (RSSI), the angle of arrival (AOA) and time of arrival (TOA). Amongst these positioning parameters, the RSSI is the least adequate for the UWB case, since it does not profit from the fine space-time resolution of impulsive signals and requires a site-specific path loss model [1].

The estimation of AOA, on the other hand, requires multiple antennas (or at least an antenna capable of beamforming) at the receiver. This requirement imply size and complexity needs that are often not compatible with the low-cost, small-size constraints associated with the typical scenarios such as wireless sensor networks, envisioned for UWB technology.

Given the reasons above, TOA stands out as the most suitable signal parameter to be used for positioning with UWB devices. Unfortunately, the estimation of the TOA of UWB signals in itself is not solved problem. For instance, correlation techniques, in conjunction with serial search, have been proposed for TOA estimation [2]. Special code design have also been considered as a means to facilitate the estimation of TOA with the correlation approach [3]. Chip-level post detection integration (CLPDI) [4]–[6], and frequency-domain approaches have also been considered [7].

All the above solutions seem, nevertheless, to be in conflict with the strict requirements of low cost and low complexity imposed on some UWB applications such as wireless sensor networks.

In order to further reduce the complexity of UWB systems, non-coherent receivers such as energy collection [8]–[10] and transmitted reference [11]–[14] have been recently proposed. In [15] an energy collection-based solution for symbol synchronization was also proposed.

This paper addresses the problem of TOA and positioning in low-cost, low-complexity UWB devices based on such energy collection approach. The key idea is to reuse the building blocks utilized in synchronization and symbol detection for TOA estimation. In addition to the some results on TOA estimation itself, the impact of these estimates on the positioning accuracy achieved by the devices is also studied.

The paper is structured as follows. In section II, a brief description of the system model is given. In section III, the two TOA estimation algorithms are defined. Simulation results are given in section IV, followed by some concluding remarks in section V.

## II. SYSTEM MODEL

In this section, a brief description of the system model is given, and general assumptions are laid out.

It is assumed that the received signal is given by the convolution of the transmitted pulse with the impulse response of the channel

$$w_{rx}(t) = w_{tx}(t) * h(t) + n(t), \quad (1)$$

where  $*$  denotes convolution,  $n(t)$  is the two-sided Gaussian noise with variance  $\sigma_n^2 = N_0/2$  and  $w_{tx}(t)$  is an arbitrary (impulsive) transmit waveform.

The channel impulse response is given by

$$h(t) = \sum_{i=1}^L \alpha_i(t) \delta(t - \tau_i), \quad (2)$$

where  $L$  is the number of the total channel paths,  $\alpha_i(t)$  and  $\tau_i$  are the amplitude and delay of the  $i$ -th path at instant  $t$ , and  $\delta(\dots)$  denotes the Dirac delta.

The detection approach is energy collection, which mathematically corresponds to the integration of the squared received signal as illustrated in figure 1. Note that the absence of correlation raises the need for a bandpass filter at the receiver, in order to minimize the effect of noise.

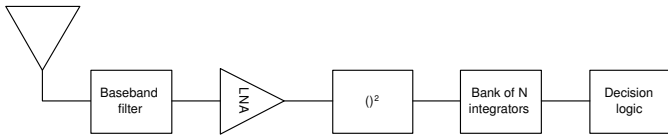


Fig. 1. Block-diagram of the non-coherent (energy collection) receiver.

### III. TOA ESTIMATION

In this section, the TOA estimation techniques considered are described. In energy collection receivers, synchronization and data detection are performed by a block of integrators. Given the constraints of low-complexity and low-cost, it is therefore appropriate consider energy collection-based TOA estimation, so as to reuse available integrators' structure.

Two major problems are faced when taking such an approach. The first is that the UWB channel is known for the fact that even in presence of a line-of-sight (LOS) scenario, the direct path is not always the strongest [16]. The second is that, in practice, the shortest integration time of an integrator unit is in the order of few hundreds of picoseconds, which implies that a single integrator often integrates over more than one channel path. For these reasons, two different algorithms have been considered for TOA estimation, namely, the *threshold-crossing* (TC) and the *maximum selection* (MAX) algorithms.

In the threshold-crossing (TC) algorithm, TOA estimation is performed by comparing the output of the integrator with a threshold. The threshold is set based on the *probability of false alarm*  $P_{fa}$ , defined as the probability that the output of integrator integrating only noise surpasses a certain level. In this method, the TOA estimate is the starting time of the first integrator that overcomes the threshold, selected with a given  $P_{fa}$  is used for . The idea is to detect the first tie the TOA estimate to the first portion of the signal energy arriving at the receiver. The drawback of this approach is that the threshold selection is crucial to the estimation accuracy. For instance, the selection of an excessively high threshold, which helps avoid false alarm, will also increased the probability of failure to detect the signal.

In the maximum selection (MAX) algorithm, the TOA is given by the starting time of the integrator giving the largest output amongst all integrators. The idea is to search for the highest cluster of energy that usually contains the direct path in the LOS channel. This approach has the advantages of avoiding signal detection failure and of being independent of issues involving the threshold selection.

In both the approaches described above, the TOA estimation resolution is bound by the size of the integration window and the signal's bandwidth. The TOA estimation is done after symbol synchronization is performed. Symbol synchronization is explained in figure 2. The pulse repetition period is divided into  $N$  integration slots (windows) and their outputs are then compared with a threshold to find the first cluster of signals reaching the receiver.

This approach gives a coarse synchronization around the starting point of the signal. The coarse synchronization provides a time reference within a range of  $\pm T_{acc}$  seconds around

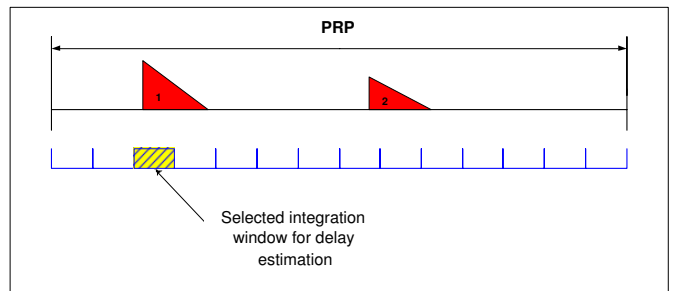


Fig. 2. Coarse synchronization scheme.

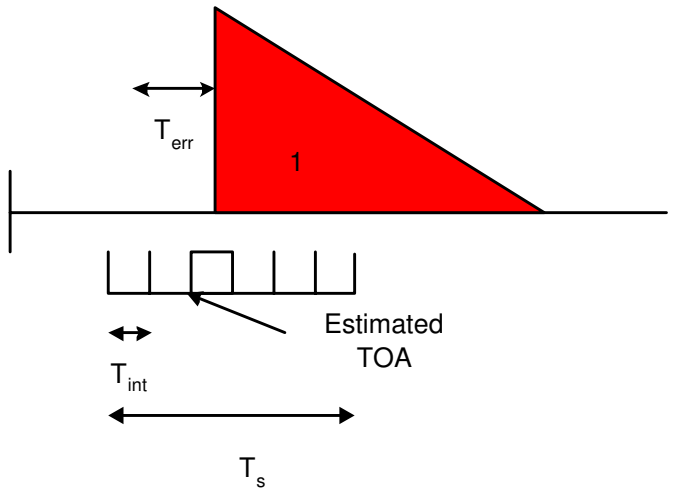


Fig. 3. TOA estimation.

the effective starting point of the data bit. The value of  $\pm T_{acc}$  depends on the integration window size and on the channel characteristics. The time window within which the TOA search is performed is defined as  $T_s = 2T_{acc} + \Delta_s$  (see figure 3), where  $\Delta_s$  represents a safety guard period that ensures that the received signal is inside the search window. The search window  $T_s$  is divided again into  $N$  integration slots defining, such that the width of a single integrator is given by  $T_{int} = T_s/N$ . The starting point of the TOA search region, denoted in figure 3 by  $T_{err}$ , lies inside the interval  $[-2T_{acc}, 0]$  and represents the coarse synchronization error.

### IV. SIMULATION RESULTS

In this section the performances of the TC and MAX algorithms are compared, both in terms of TOA estimation error and positioning accuracy.

Simulations are done utilizing the Saleh Valenzuela channel model 3 (CM3) and channel model 4 (CM4) as defined in the IEEE 802.15.4a standard for indoor office environment [17]. CM3 includes a LOS path (corresponding to the shortest time of arrival) in all channel realizations, but the this first path is not always the strongest in the whole impulse response. CM4 is a non line-of-sight channel model.

The pulse width considered in this paper is 0.5 ns, which results in a signal bandwidth of 4 GHz at  $-10$  dB.

This bandwidth corresponds to the bandwidth of the band-pass filter used by the receiver. Perfect synchronization between transmitter and receiver clocks is assumed.

The simulation parameters are as follows:  $T_{acc} = 7.5$  ns;  $\Delta_S = 5$  ns, which implies  $T_s = 20$  ns;  $T_{err}$  is a random in limited to the interval  $[-T_u, 0]$ , are  $T_u = 2T_{acc}$ ; the number of integrators considered are 5, 10 and 20, respectively defining the integration windows  $T_{int}$  of 4, 2 and 1 ns.

For the TC algorithm the threshold is set using several integration values obtained in the integration window  $T_{int}$  when only noise is present. In figure 4 and 5 the distributions of the delay estimation error are plotted for both MAX and TC algorithms considering a number of integrators  $N = 10$ .

Noise and integration time bigger then pulse width are, for both the algorithms, the reasons of under estimating the TOA value.

The TC algorithm is less sensitive to the energy distribution inside the multipath channel showing a steeper decay in the region of the over estimated TOA values.

As shown in figure 6 for low  $E_b/N_0$  the TC algorithm is strongly affected by the  $P_{fa}$ . The reduction of the  $P_{fa}$  produces better performance in terms of TOA error but increases the probability of missed detection  $P_m$ . Figure 7 shows that TC algorithm gives good result for relatively high values of  $E_b/N_0$  outperforming the MAX algorithm, as it is shown in figure 5.

Both algorithms benefit from an augmented number of integrators reducing the probability of under estimating the delay. On the other hand this increase in number of integrators produce a slight increase of the probability to over estimate the delay. Moreover from figures 8 and 9 it can be noticed that, passing from 5 to 10 integrators brings to a substantial improvement of the TOA error distribution profile. This improvement is more evident for TC then MAX algorithm. A further increase in the number of integrators from 10 to 20 brings only a negligible change. To be noticed that for the TC algorithm to an augmented number of integrators corresponds a slight increase of the false alarm occurrence.

To have an idea how this TOA estimation can effect the positioning algorithm, different spherical scenarios of radius  $R$  have been considered. In each of this scenarios 4 fixed nodes and 1 device are present. The 4 fixed nodes estimate the TOA of the signal coming from the device and then based on the 4 delay estimations the position of the device is calculated. For each device-fixed node link a different channel realization is considered. The position of the fixed nodes and the position of the device are taken randomly inside the sphere of radius  $R$  for each simulation run.

For positioning calculation the Davidon-Fletcher-Powell (DFP) quasi-Newton algorithm is used. The DFP algorithm has already been study for UWB system [18] and implemented in a UWB commercialized solution for location system [19]. Being the DFP an iterative algorithm, the performance are expected to improves increasing the number of iteration. The results presented here are obtained with a single iteration.

The received signal power in each fixed node is calculated

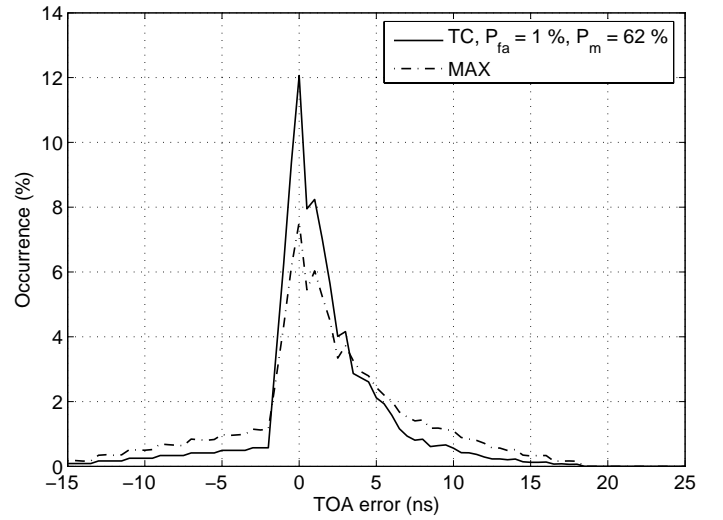


Fig. 4. Comparison between MAX and TC algorithm.  $T_u = 15$  ns,  $N = 10$ ,  $T_{int} = 2$  ns and  $E_b/N_0 = 10$  dB.

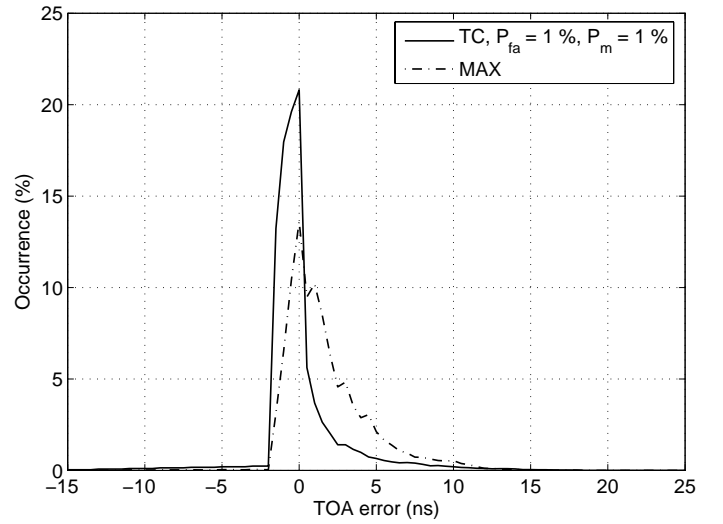


Fig. 5. Comparison between MAX and TC algorithm.  $T_u = 15$  ns,  $N = 10$ ,  $T_{int} = 2$  ns and  $E_b/N_0 = 20$  dB.

based on the link budget formula as follows

$$P_r = P_t + G_t + G_r + L_f + L_d - 10 \log(D_r) - (KT_b - F) - I \quad (3)$$

where the value  $P_t = -5.28$  dBm represents the maximum allowed transmittable signal power in the FCC mask in a bandwidth of 4 GHz,  $G_t = 0$  dB and  $G_r = 0$  dB are the gains of the antennas at the transmitter and receiver side,  $L_f = 20 \log(4\pi f_c / 3 \cdot 10^8)$  is the free space path-loss for a central frequency  $f_c = 4.1$  GHz,  $L_d = 10\alpha \log(d)$  is the loss due to the distance  $d$ , with  $\alpha$  coefficient of attenuation and  $\alpha = 1.79$  and  $\alpha = 3.06$  respectively for CM3 and CM4,  $D_r = 11$  Mbit/s is the data rate,  $KT_b = -173$  dB is the Boltzman constant for temperature of 300 K,  $F = 7$  dB is the noise figure and  $I = 1$  dB takes in to account the implementation loss. Figure 10 reports the positioning mean absolute error in meter (m) respectively considering

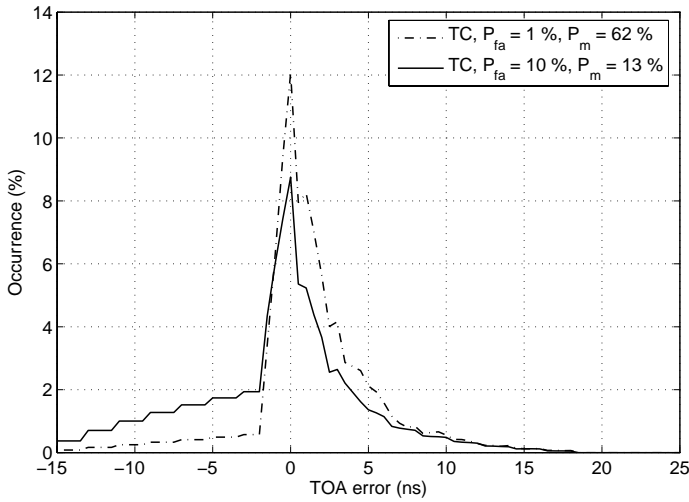


Fig. 6. TC algorithm.  $T_u = 15$  ns,  $N = 10$ ,  $T_{int} = 2$  ns and  $E_b/N_0 = 10$  dB.

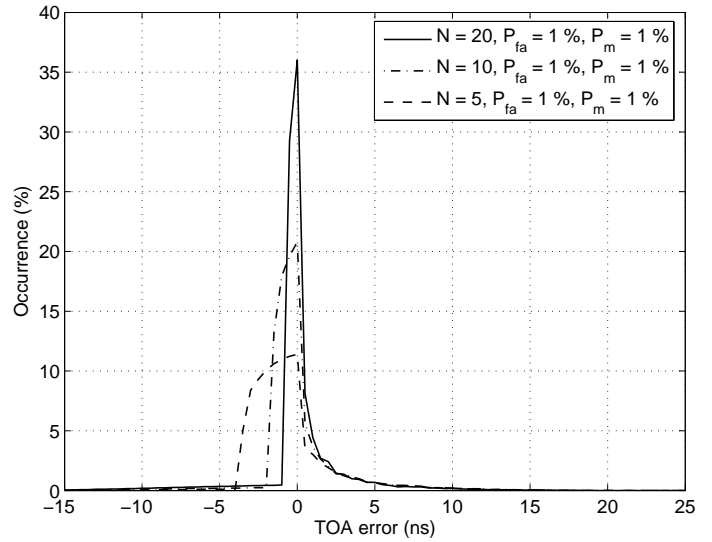


Fig. 8. TC algorithm.  $T_u = 15$  ns,  $P_{fa} = 1\%$  and  $E_b/N_0 = 20$  dB.

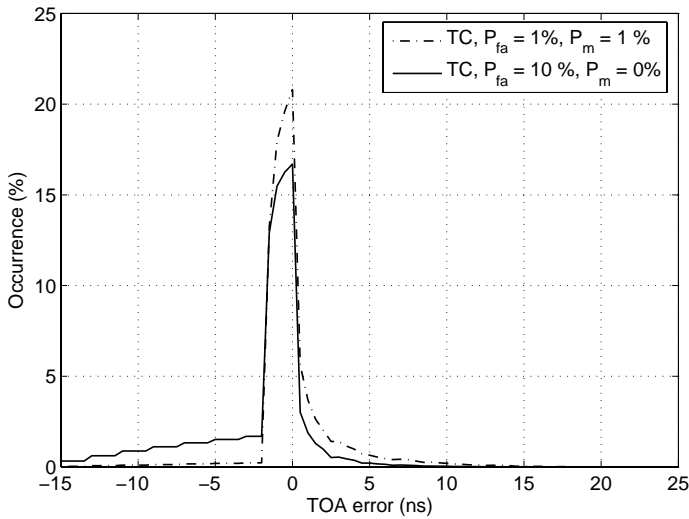


Fig. 7. TC algorithm.  $T_u = 15$  ns,  $N = 10$ ,  $T_{int} = 2$  ns and  $E_b/N_0 = 20$  dB.

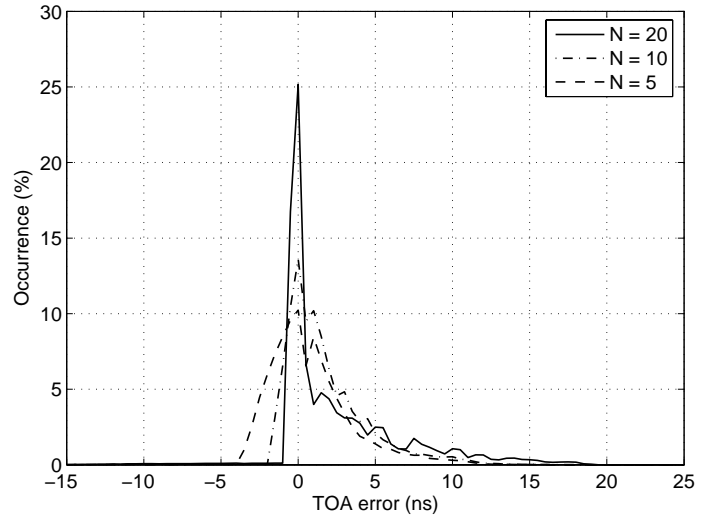


Fig. 9. MAX algorithm.  $T_u = 15$  ns and  $E_b/N_0 = 20$  dB.

TC algorithm for  $P_{fa} = 10\%$  and  $P_{fa} = 1\%$ , and MAX algorithm. The results are for  $R$  values of 5, 10, 15, 20, and 30 meters. The increase in number of integrators seems to produce not a relevant improvement for MAX while for TC with  $P_{fa} = 10\%$  the increase of  $N$  produces a performance degradation due to the high false alarm occurrence. Differently an improvement is present when the TC algorithm is used with  $P_{fa} = 1\%$  and the number of integrators passes from 5 to 10. This improvement is explained by the result obtained with the TOA estimation. The best positioning error obtained are result on the order of 10% of the radius of the spherical environment for  $R$  up to 30 m.

Figure 11 reports the positioning mean absolute error considering that the device is in LOS with 3 fixed nodes and in NLOS with 1 fixed node. Comparing figure 10 and 11, a small degradation of the performance is visible when there is a NLOS situation. The degradation is more accentuate for

#### MAX selection algorithm.

In figures 10 and 11, the probability of a failed calculation, due to a missed detection of the TC algorithm, is not shown. However, this probability drastically increases when the link distance increases.

Assuming that the fixed node knows a rough estimate of the link distance and it has the capability to choose between TC and MAX algorithms, it can be seen that the TC algorithm is the best option for short link distances and the MAX algorithm is the best option for short link distances. This is because for short link distances, the TC algorithm offers better TOA performance with very small probability of missed detection. For longer link distances the performance of the MAX algorithm is quite close to that of the TC algorithm but with zero probability of missed detection.

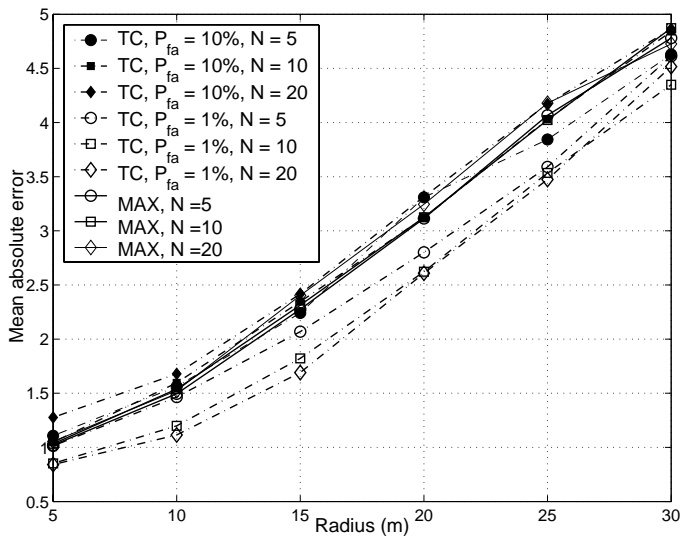


Fig. 10. Positioning mean absolute error obtained using the DFP positioning algorithm with a single iteration in 802.15.4a CM3(LOS) environment

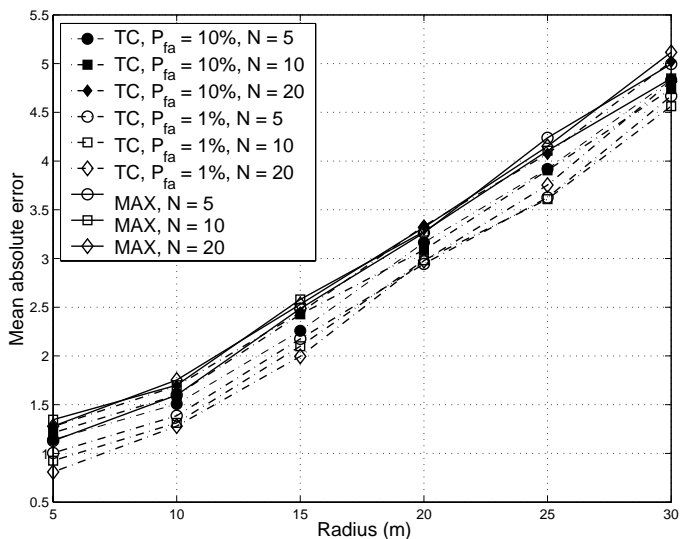


Fig. 11. Positioning mean absolute error obtained using the DFP positioning algorithm with a single iteration in 802.15.4a CM3(LOS) and CM4(NLOS) mixed environment.

## V. CONCLUSION

In this paper, two TOA estimation techniques have been investigated for a non coherent, energy collection UWB receiver.

Two different algorithms, TC and MAX have been considered and compared. With accurate threshold setting and high SNR, the TC algorithm outperforms the MAX algorithm. The TC algorithm however has relatively high levels of missed detection for low SNR values. The MAX algorithm appears to be more robust to SNR value changes.

The performance of the algorithms in terms of positioning accuracy have been also presented considering the DFP algorithm. The results show that the energy collection technique is an appropriate solution for TOA estimation in low complexity

UWB systems.

## ACKNOWLEDGEMENT

This work has been supported by the European Integrated Project PULSERS [20]. The authors would like to thank the partners.

## REFERENCES

- [1] Xinrong Li, *Super-Resolution TOA Estimation with Diversity Techniques for Indoor Geolocation Applications*, Ph.D. thesis, Worcester Polytechnic Institute, 2003.
- [2] E. A. Homier and Robert A. Scholtz, "Rapid acquisition of ultra-wideband signals in the dense multipath channel," in *Proc. IEEE 2<sup>nd</sup> Ultra Wideband Systems and Technologies (UWBST'02)*, May 2002, pp. 245–249.
- [3] R. Fleming, C. Kushner, G. Roberts, and U. Nandiwada, "Rapid acquisition for ultra-wideband localizers," in *Proc. IEEE 2<sup>nd</sup> Ultra Wideband Systems and Technologies (UWBST'02)*, May 2002, pp. 105–109.
- [4] J. Iinatti and M. Latva-aho, "A modified CLPDI for code acquisition in multipath channel," in *Proc. IEEE Personal, Indoor and Mobile Radio Communications (PIMRC'01)*, Sept. 2001, vol. 2, pp. F–6 F–10.
- [5] S. Soderi, J. Iinatti, and M. Hamalainen, "CLPDI algorithm in UWB synchronization," in *Proc. IEEE 1<sup>st</sup> International Workshop of UWB Systems (IWUWBS'03)*, June 2003.
- [6] I. Oppermann, M. Hämäläinen, and J. Iinatti, *Ultra wideband theory and applications*, Wiley & Sons, Ltd., 2004.
- [7] I. Maravic, M. Vetterli, and K. Ramchandran, "Channel estimation and synchronization with sub-nyquist sampling and application to ultra-wideband systems," in *In Proc. IEEE Symposium on Circuits and Systems (ISCAS)*, Vancouver, Canada, May, pp. 381–384.
- [8] M. Weisenhorn and W. Hirt, "Robust noncoherent receiver exploiting UWB channel properties," in *Proc. Joint UWBST&IWUWBS*, May 2004, vol. 2, pp. 156–160.
- [9] Y.P. Nakache, P. Orlik, W.M. Gifford, A.F. Molisch, I. Ramchandran, G. Fang, and Jinyun Zhang, "Low-complexity ultrawideband transceiver with compatibility to subband-OFDM," in *Proc. Joint UWBST&IWUWBS*, May 2004, pp. 151–155.
- [10] A. Rabbachin, R. Tesi, and I. Oppermann, "Bit error rate analysis for UWB systems with a low complexity, non-coherent energy collection receiver," in *Proc. IST Mobile & Wireless Communications Summit*, Lyon, France, June 2004, vol. 2.
- [11] T. Q. S. Quek and M. Z. Win, "Ultrawide bandwidth transmitted-reference signaling," in *Proc. IEEE International Conference on Communications (ICC)*, June 2004, vol. 6, pp. 3409–3413.
- [12] R. Hocht and H. Tomlinson, "Delay hopped transmitted reference experimental results," in *Proc. IEEE 2<sup>nd</sup> Ultra Wideband Systems and Technologies (UWBST'02)*, May 2002, pp. 93–98.
- [13] R. Hocht and H. Tomlinson, "Delay-hopped transmitted-reference RF communications," in *Proc. IEEE 2<sup>nd</sup> Ultra Wideband Systems and Technologies (UWBST'02)*, May 2002, pp. 265–269.
- [14] J. D. Choi and W. E. Stark, "Performance of ultra-wideband communications with suboptimal receivers in multipath channels," *IEEE J. Select. Areas Commun.*, vol. 20, pp. 1754–1766, Dec. 2002.
- [15] A. Rabbachin and I. Oppermann, "Synchronization analysis for UWB systems with a low-complexity energy collection receiver," in *Proc. Joint UWBST&IWUWBS*, May 2004, pp. 288–292.
- [16] Lee Joon-Yong and R. A. Scholtz, "Ranging in a dense multipath environment using an uwb radio link," *IEEE J. Select. Areas Commun.*, vol. 20, pp. 1677 – 1683, Dec. 2002.
- [17] "IEEE 802.15.4a channel model - final report," <http://www.ieee802.org/15/pub/TG4a.html>.
- [18] K. Yu and I. Oppermann, "Performance of uwb position estimation based on time-of-arrival measurements," in *Proc. Joint UWBST&IWUWBS*, May 2004, pp. 400 – 404.
- [19] R. J. Fontana, E. Richley, and J. Barney, "Commercialization of an ultra wideband precision asset location system," in *Proc. IEEE 3<sup>rd</sup> Ultra Wideband Systems and Technologies (UWBST'03)*, Nov. 2003, pp. 369–373.
- [20] "PULSERS: Pervasive ultra-wideband low spectral energy radio systems," <http://www.pulsers.net/index2.html>.